Peptides 79 (2016) 75–82

Contents lists available at ScienceDirect

Peptides

journal homepage: www.elsevier.com/locate/peptides

Antimicrobial properties of two novel peptides derived from *Theobroma cacao* osmotin

Loeni L. Falcao[a], Joseilde O. Silva-Werneck[a], Alessandra de R. Ramos[b], Natalia F. Martins[a], Emmanuel Bresso[a], Magali A. Rodrigues[c], Marcelo P. Bemquerer[a], Lucilia H. Marcellino[a,*]

[a] *Embrapa Genetic Resources and Biotechnology, Brasília, DF, Brazil*
[b] *Federal University of the South and Southeast of Pará (Unifesspa), Pará, Brazil*
[c] *Centro Universitário Planalto do Distrito Federal (Uniplan), Brasília, DF, Brazil*

ARTICLE INFO

Article history:
Received 9 December 2015
Received in revised form 10 March 2016
Accepted 11 March 2016
Available online 17 March 2016

Keywords:
Antimicrobial peptide
Osmotin-like protein
Pathogenesis-related
Antifungal activity
Phytopathogens
Yeast
Cacao
Moniliophthora perniciosa

ABSTRACT

The osmotin proteins of several plants display antifungal activity, which can play an important role in plant defense against diseases. Thus, this protein can be useful as a source for biotechnological strategies aiming to combat fungal diseases. In this work, we analyzed the antifungal activity of a cacao osmotin-like protein (TcOsm1) and of two osmotin-derived synthetic peptides with antimicrobial features, differing by five amino acids residues at the N-terminus. Antimicrobial tests showed that TcOsm1 expressed in *Escherichia coli* inhibits the growth of *Moniliophthora perniciosa* mycelium and *Pichia pastoris* X-33 *in vitro*. The TcOsm1-derived peptides, named Osm-pepA (H-RRLDRGGVWNLNVNPGTTGARVWARTK-NH_2), located at R23-K49, and Osm-pepB (H-GGVWNLNVNPGTTGARVWARTK-NH_2), located at G28-K49, inhibited growth of yeasts (*Saccharomyces cerevisiae* S288C and *Pichia pastoris* X-33) and spore germination of the phytopathogenic fungi *Fusarium f. sp. glycines* and *Colletotrichum gossypi*. Osm-pepA was more efficient than Osm-pepB for *S. cerevisiae* (MIC = 40 μM and MIC = 127 μM, respectively), as well as for *P. pastoris* (MIC = 20 μM and MIC = 127 μM, respectively). Furthermore, the peptides presented a biphasic performance, promoting *S. cerevisiae* growth in doses around 5 μM and inhibiting it at higher doses. The structural model for these peptides showed that the five amino acids residues, RRLDR at Osm-pepA N-terminus, significantly affect the tertiary structure, indicating that this structure is important for the peptide antimicrobial potency. This is the first report of development of antimicrobial peptides from *T. cacao*. Taken together, the results indicate that the cacao osmotin and its derived peptides, herein studied, are good candidates for developing biotechnological tools aiming to control phytopathogenic fungi.

1. Introduction

Theobroma cacao L. is an important commodity affected by several fungal diseases that result in heavy production losses [1]. One of the most important is witches' broom disease, caused by the basidiomycete *Moniliophthora perniciosa*, that severely attacks cacao plantation in Brazil, which is ranked among the world's biggest cocoa producers [2]. Cacao and fungal genome studies have been performed [3–5] and are helping to understand plant-pathogen interactions. Several pathogenesis-related proteins (PR) have been identified in the cacao's genome, among them osmotin, a protein that belongs to the PR-5 family and is widely found in plants. Generally, it plays a role in the adaptation of the plant to adverse conditions and defense against diseases, being induced by biotic or abiotic stress stimuli [6]. Osmotin was first described in *Nicotiana tabacum*, where it accumulates as a function of osmotic adaptation [7]. Since then, several osmotin-like proteins were shown to have antifungal activity against a broad range of fungi *in vitro*, as well as in transgenic plants. As an example, leaves of transgenic potato plants expressing tobacco osmotin exhibited partial resistance to *Phytophtora infestans* [8]. The tertiary structure of osmotin from several sources has been determined. In general, the protein has been shown to be a three-domain structure, containing an acidic cleft between domains I and II, which is potentially involved in a

Abbreviations: AMP, antimicrobial peptide; Boc, t-butyloxycarbonyl; CFU, colony forming unit; DAI, days after inoculation; HOBt, 1-hydroxybenzotriazol; MIC, minimal inhibitory concentration; Pbf, 2,2,4,6,7-pentamethyl-3H-1-benzofuran-5-sulfonyl; PMSF, phenylmethanesulfonyl fluoride; PR, pathogenesis-related protein; tBu, t-butyl; Trt, triphenylmethyl.

* Corresponding author.
E-mail address: lucilia.marcellino@embrapa.br (L.H. Marcellino).

http://dx.doi.org/10.1016/j.peptides.2016.03.006
0196-9781/

catalytic activity of β 1,3 glucan, a component of fungi cell wall, what could explain its antifungal properties [6]. However, some other mechanism is possibly involved. Other studies demonstrated that osmotin is recognized by a membrane receptor, triggering a pathway that results in ROS (reactive oxygen species) accumulation, leading to cell death [9], but the actual mechanism(s) remains unclear. Due to its characteristics, this protein can be exploited to achieve resistance to fungal diseases in plants by biotechnological means.

One possibility is to explore the protein as a source of antimicrobial peptides due to its antifungal activity [6]. Biologically active peptides, such as antimicrobials, neuroactive and immunologically active molecules, inserted as cryptic sequences into proteins of diverse functions, are well known. They are normally found in abundant proteins, such as hemoglobin and casein [10–12]. Antimicrobial peptides are predominantly cationic, amphiphilic and many of them are helicoidal, making the prediction of antimicrobial activity of a given peptide feasible [13,14]. Considering these characteristics, AMPs are being discovered through sequence searches within proteins from animals and plants [15,16]. Brand and collaborators (2012), searching for intragenic antimicrobial peptides in soybean proteins, have found two peptides with antimicrobial activity against *Xanthomonas axonopodis* pv. *glycines*, the causal agent of the bacterial pustule disease, and the fungus *Phakopsora pachyrhizi*, the causal agent of the soybean Asian rust.

The aims of the present study are to characterize an osmotin-like protein from *T. cacao* (TcOsm1) regarding its antifungal activity, as well as to identify cryptic AMPs in the protein sequence, and to investigate the effectiveness of these AMPs as antifungal agents.

2. Material and methods

2.1. Source and growth of microorganisms

Saccharomyces cerevisiae S288C [17] and *Pichia pastoris* X-33 (Invitrogen, CA, USA) were kindly donated by Dr. Lidia Pepe de Moraes (University of Brasilia, Brazil). They were grown at 28 °C, 180 rpm, overnight, in 25 mL of YG medium (5 g/L yeast extract, 25 g/L D-glucose) from a pre-culture. *Fusarium solani f. sp. glycines* and *Colletotrichum gossypii* were kindly donated by Dr. Marilia Santos Silva (Embrapa, Brazil). *M. perniciosa* was kindly donated by Dr. Alessandra de Rezende Ramos (UNIFESSPA—Federal University of the South and Southeast of Pará, Brazil). All fungi were grown on PDA medium (4 g/L potato extract, 20 g/L dextrose, 15 g/L agar), at 28 °C, and stored at 4 °C.

2.2. Antimicrobial peptide prediction

The conserved motifs present in TcOsm1 sequence were identified by MotifMaker online tool (http://landau.utmb.edu:8080/pcpmer//Tools/SubmitFormMotifMaker.jsp). The search for sequences with antimicrobial propensity was conducted by searching for segments with interspersed hydrophobic and cationic residues in the TcOsm1 primary sequence, followed by verification at the antimicrobial peptide database (http://aps.unmc.edu/AP/prediction/prediction_main.php).

2.3. Antimicrobial peptide synthesis

The peptides H-RRLDRGGVWNLNVNPGTTGARVWARTK-NH_2 and H-GGVWNLNVNPGTTGARVWARTK-NH_2 were synthesized by the Fmoc (Fluorenyloxycarbonyl) solid phase method [18], starting from "Rink-amide-MBHA resin" (0.52 mmol/g). The amino acid derivatives with side-chain protecting groups were the following: Fmoc-Arg(Pbf)-OH, Fmoc-Asp(OtBu)-OH, Fmoc-Trp(Boc)-OH, Fmoc-Asn(Trt)-OH, Fmoc-Thr(tBu)-OH, Fmoc-Lys(Boc)-OH. Fmoc group removal was performed with 4-methylpiperidine in *N,N*-dimethylformamide (DMF) at 25% (v/v) for 30 min (two steps of 15 min). The couplings for peptide bond formation were conducted with 1,2-diisopropylcarbodiimide (DIC)/1-hydroxybenzotriazole (HOBt), or DIC/2-cyano-2-(hydroxiimino) ethyl acetate [19] in DMF during 60–120 min. After the deprotection and coupling steps, the peptidyl-resin was washed three times with 2-propanol followed by DMF. The deprotection and coupling reactions were monitored by the ninhydrin reaction, even for proline residues [20,21]. After the synthesis was completed, the final deprotection reaction and cleavage of the peptide from the resin were performed with 10 mL of a solution containing trifluoroacetic acid (TFA), triisopropylsilane (TIS) and water—TFA:TIS:water (90:5:5, v:v:v) for 90 min, at 25 °C. After four washings with cold diisopropyl ether, the supernatant was discharged and the peptide was extracted with water, and freeze-dried. For the purification of the peptide, a semi-preparative column (ODS 9.4 × 250 mm) from Agilent (Santa Clara, CA) was used, in a LC-10 model (Shimadzu, Kyoto, Japan) chromatographer. The gradient used was as follows: water:acetonitrile:TFA (95:5:0.1, v:v:v) for 5 min, followed by a linear gradient up to water:acetonitrile:TFA (35:65:0.1, v:v:v) for 60 min. The detection was performed at 216 and 280 nm and the flow rate was 3.0 mL/min, at 25 °C. The identity and degree of purity of the peptide was verified by MALDI-ToF mass spectrometry, by using α-cyano-4-hydroxycinnamic acid as a matrix. The spectra were acquired in an Ultraflex III ToF–ToF (Bruker Daltonics, Bilerica, MA), in reflected mode. Peptide fragmentation by MS/MS was conducted through the LIFT™ methodology [22]. The purity of the peptides was higher than 97% as evaluated by liquid chromatography and MALDI-MS. Stock solutions of the peptides were prepared in water and concentrations were determined accordingly to the Murphy & Kies method [23]

2.4. Subcloning of osm1 in expression vector pQE-30

The *osm1* gene (AY766059.2), previously cloned into pGEM-T Easy (Promega, Madison, WI), was amplified by using the primers OsmBamHI—5′GCCGGATCCGCCACTATTA3′ and OsmHindIII: 5′GATTCAAAGCTTCCTCAAGG3′. The resulting fragments were cloned into the *Bam*HI/*Hin*dIII sites of the expression vector pQE-30 Xa (Qiagen, Valencia, CA), generating the recombinant plasmid named pQE-osm, in which *osm1* is fused in frame to the His_6 tag-coding region. The recombinant plasmid was inserted into *E. coli* strain M15 [pREP4] obtaining the clone pQE-osm. The vector pQE-30 Xa was used as control.

2.5. Expression of the gene osm1

For production of TcOsm1 protein, the strain pQE-osm was cultured at 37 °C, 200 rpm, and induced by 1 mM IPTG (isopropyl-β-D-thiogalactopyranoside) for 4 h. The cells were harvested, ressuspended in 25 mL of Lysis buffer (25 mM Tris-HCl pH 7.4, 10 mM NaCl, 1 mM DTT, 1 mM PMSF, 0.1 mg/mL lysozyme) and incubated at 37 °C, for 30 min, with gentle agitation. The cells were sonicated (10 s on/10 s off, Branson 102C sonicator, Danbury, CT) and, after centrifugation (11,000*g* for 30 min at 4 °C), the supernatant was dialyzed (Spectrapor membrane tubing, 2 mL/cm, dry cylinder 15.9 mm diameter, mwco 12–14,000—Thomas Scientific, Swedesboro, NJ, USA) against dialysis buffer (25 mM Tris-HCl, pH 7.4, 10 mM NaCl). The dialyzed soluble proteins were filtered through a 0.22 μm membrane (TPP, Techno Plastic Products AG, Switzerland). The proteins were quantified by the method of Bradford [24], using Bio-Rad Protein Assay reagent (Bio-Rad, Hercules, CA, USA) and bovine serum albumin (BSA) as a standard. The proteins were analysed by 13.5% SDS-PAGE [25].

To confirm the presence of the fusion protein (His-Osm) in the protein extract of the induced culture of pQE-osm, immunodetection was performed by Western blotting, according to Sambrook and collaborators [26] with slight modifications. Briefly, the proteins were separated by 13.5% SDS-PAGE, then transferred to a PVDF membrane (Hybond-P, 0.45 μm, Amersham-Pharmacia-GE Biotec, Waukesha, WI) through a Mini trans-blot electrophoretic transfer cell (Bio-Rad), at 170 V, for two hours. The membrane was blocked with 5% skimmed milk in TBS (20 mM Tris-HCl, pH 7.5, 150 mM NaCl) plus 0.05% Tween 20, for 1 h, at 25 °C, and then incubated in Anti-His antibody (GE Healthcare, Waukesha, WI) diluted 1:3000 in incubation solution (TBS, 0.05% Tween 20, 3% skimmed milk) for 1 h, at 25 °C, with gentle agitation. After three brief washings in TTBS (TBS, 0.1% Tween 20), it was incubated in secondary antibody conjugated with alkaline phosphatase ["Anti-mouse IgG (whole molecule) alkaline phosphatase conjugate (goat)", Sigma-Aldrich, St Louis, MO] diluted 1:2000 in incubation solution, for 1 h, at 25 °C, with gentle agitation. Following three washings in TTBS, colorimetric detection was performed using the Alkaline Phosphatase Conjugate Substrate Kit (Bio-Rad, Hercules, CA), at 25 °C, according to the manufacturer's instructions.

2.6. Antimicrobial tests

2.6.1. Osmotin

Different amounts (15, 30 and 37 μg/cm^2) of the dialyzed and filtered soluble proteins of the induced pQE-osm clone, as well as the control clone, were added to the surface of PDA medium (4 g/L potato extract, 20 g/L dextrose, 15 g/L agar) in 5-cm diameter Petri dishes. After surface drying, a 0.5-cm diameter disc of *M. perniciosa* mycelium was placed at the center of each plate. The treatments were done in triplicate. The plates were incubated at 28 °C for 21 days. Mycelial growth was accessed by taking the average of two perpendicular diameters (in cm), on the 21st day. The *M. perniciosa* growth was evaluated as a percentage relatively to the control (pQE-30 proteins). Statistical analysis was performed according to the Tukey test (R package).

The tests with *P. pastoris* X-33 were performed in 96 wells plates, in 100 μL assay, containing 40 μL of yeast suspension (10^4 CFU/mL) in modified YG medium (5 g/L yeast extract, 12.5 g/L D-glucose), and 60 μL of the soluble proteins from the induced pQE-osm clone, or the control pQE30 clone, in dialysis buffer. The proteins were tested at concentrations of 0.12, 0.23, 0.45 and 0.9 μg/μL, in triplicate. Dialysis buffer was used as a control. The plate was initially incubated for 6 h at 28 °C, 180 rpm. Then, it was further incubated for 40 h, without shaking, in a Spectra Max 190 microplate reader (SMolecular Devices, Sunnyvale, CA, USA), recording the absorbance at 650 nm every 30 min. The bioassay was repeated three times.

2.6.2. Peptides

The tests with *S. cerevisiae* S288C and *P. pastoris* X-33 were performed in 96 wells plates, in 100 μL assay, containing 20 μL of AMP solution and 80 μL of the yeast cells suspension (10^4 CFU/mL) in YG medium. The final peptide concentrations ranged from 1.25 to 80 μM for Osm-pepA and 5.0–127 μM for Osm-pepB, which were two fold serially diluted in water. The treatments were performed in triplicate. In the negative control, no AMP was added. The assay was conducted at 28 °C for 24 h, without shaking, with absorbance at 650 nm being recorded every 15 min, using a Spectra Max 190 microplate reader (SMolecular Devices, Sunnyvale, CA USA). The MIC was determined by recording the lowest concentration of the peptide that prevented detectable growth of the microorganism at 20 h of assay. The bioassay was repeated three times.

The test with *F. solani f. sp. glycines* and *C. gossypii* was performed in 1.5 mL tubes, in 100 μL assay, containing 50 μM Osm-pepA and 100–150 viable spores in 10 mM PBS (sodium phosphate buffer), pH 7.4, in triplicate. A negative control was performed without AMP. After incubation at 28 °C for 24 h, the treated spores were spread on PDA medium plates and incubated at 28 °C, for 24 h for *F. solani f. sp. glycines* and 48 h for *C. gossypii*. The antimicrobial effect was evaluated by the number of colonies formed. The bioassay was repeated three times for *F. solani f. sp. glycines* and twice for *C. gossypii.*

The test with *M. perniciosa* was performed by placing a 0.5-cm diameter mycelial disc on the surface of PDA medium containing 100 μM Osm-pepA, in a 3.5-cm diameter Petri dish, in triplicate. After incubation at 28 °C for 13 days, the antimicrobial effect was accessed by taking the average of two perpendicular diameters (in cm) of the mycelium. The bioassay was repeated twice.

2.7. Tertiary structure prediction

2.7.1. Homology modeling

To predict the three dimensional structure of TcOsm1, a preliminary 3D model was generated by computer-aided molecular modeling. First, searches for similar structures were carried out through BLAST at the protein database (PDB) in order to detect which proteins would be a suitable template for both structure and function. Then, the model was generated by the PS^2 structure prediction server [27], using the template 1Z3Q chain A, an antifungal banana fruit thaumatin-like protein with 80.6% identity with TcOsm1. This model was refined by molecular dynamics simulations.

2.7.2. Molecular dynamics

The protein was first solvated in a 80 Å^3 box of explicit water molecules plus nine chloride ions to ensure electrostatic neutrality. The NAMD2 program [28] was employed with the CHARMM27 force field in the simulation of 40,217 atoms ensemble. The energy minimization task was achieved by 6400 steps of conjugate gradients. The conformational behavior of the whole system was obtained by running 10 ns of MD. Periodic boundary conditions were used for an NPT ensemble (number of particles N, pressure P and temperature T) at a temperature of 300 K and 1 atm pressure. A frame was recorded from the MD simulation each ps so that an ensemble of 10,000 frames was finally obtained from the whole simulations. From this frame ensemble, the conformational behavior of the protein was analyzed using several programs attached as plugins to VMD.

3. Results

3.1. Effect of cacao osmotin on M. perniciosa mycelium and yeast growth

In order to evaluate the antifungal effect of TcOsm1 on *M. perniciosa*, the protein expressed in *E.coli* was used. The *osm1* gene, cloned in pQE-osm downstream 6XHis-Tag, was expressed in *E. coli* M15[pREP4] upon IPTG induction. Analysis by SDS-PAGE and immunoblotting confirmed the presence of TcOsm1 in the soluble protein fraction of the induced culture, which presented a protein band around 23 kDa, expected for the His-Osm fusion. Some higher bands were also detected and can correspond to protein dimers and trimers (Fig. 1). This protein was not observed among proteins of the non-induced pQE-osm culture, neither in the control pQE-30 cultures (Fig. 1). TcOsm1 was also present in the insoluble fraction of the induced pQE-osm culture (data not shown).

Following the detection of TcOsm1 in the soluble protein fraction of *E. coli* extracts (Fig. 1), it was tested against *M. perniciosa* and the yeasts *S. cerevisiae* and *P. pastoris*. In the presence of TcOsm1, the growth of *M. perniciosa* was reduced in a dose-dependent manner (Fig. 2A). The mycelial diameters of the colonies treated with

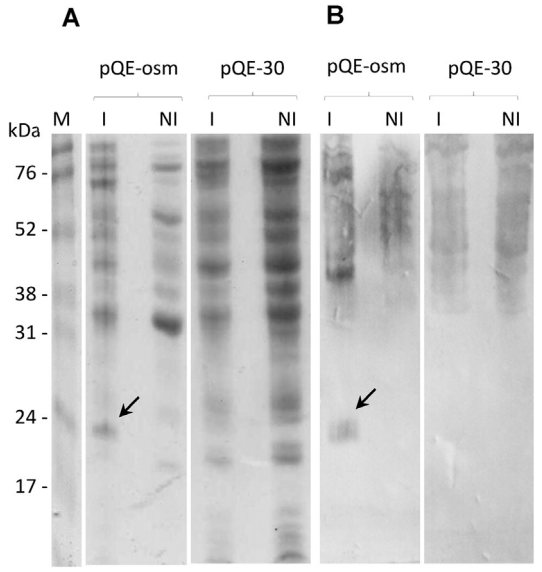

Fig. 1. Analysis of TcOsm1 expression in *E. coli*. (A) SDS-PAGE 13.5% analysis of soluble proteins of induced (I) or non-induced (NI) cultures of *E. coli* cells harboring pQE-osm vector or the control pQE-30 vector. (B) Immunoblotting using anti-His antibody. Arrows indicate expressed TcOsm1.

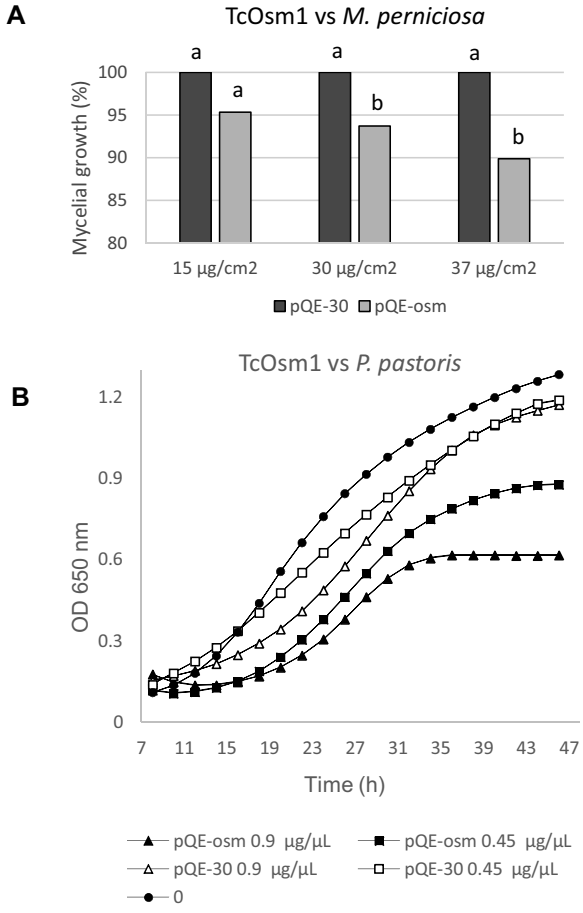

Fig. 2. Effect of TcOsm1 on *Moniliophthora perniciosa* and *Pichia pastoris* growth. (A) Growth of *M. perniciosa* mycelium treated with expressed TcOsm1. Soluble proteins from pQE-osm clone were applied on PDA at 15, 30 and 37 µg/cm^2, and the *M. perniciosa* growth was evaluated relatively to the control (pQE-30 proteins) at 21 DAI. Significantly different values ($p < 0.05$), according to the Tukey test (R package), are indicated by different letters (a and b). (B) Growth of *P. pastoris* treated with expressed TcOsm1. Soluble proteins from pQE-osm and the control pQE-30 were added to YG medium. The graph shows the growth curves for the higher concentrations used (0.45 and 0.9 µg/µL).

proteins from pQE-osm were smaller than those treated with proteins from the control pQE-30 clone, being statistically significant ($p < 0.05$) at 30 and 37 µg/cm^2 with about 6 and 10% reduction, respectively. Regarding yeasts, preliminary results indicated that TcOsm1 was not active against *S. cerevisiae* (data not shown). For *P. pastoris*, the proteins were tested in a range from 0.12 to 0.9 µg/µL. The strongest effects on its growth were observed with pQE-osm proteins at 0.45 and 0.9 µg/µL, while the other concentrations did not seem to have caused significant growth reduction (Fig. 2B).

3.2. TcOsm1-derived synthetic peptides: prediction and antifungal activity

Analysis of *T. cacao* osmotin revealed that it contains a region, corresponding to domain I, presenting antimicrobial peptide features. Two peptides in this domain were synthesized for further studies: (a) RRLDRGGVWNLNVNPGTTGARVWARTK, with amidated C-terminus, named Osm-pepA, presenting molecular weight of 3050.5 g/mol and +6 net charge at pH 7, calculated using pepcalc tool (http://pepcalc.com/). (b) GGVWNLNVNPGTTGARVWARTK, with amidated C-terminus, named Osm-pepB, with molecular weight of 2353.7 g/mol, and +4 net charge at pH 7.

The antifungal activity of Osm-pepA and Osm-pepB was initially evaluated against *S. cerevisiae* and *P. pastoris*. These yeasts were treated with Osm-pepA and Osm-pepB at different concentrations and their growth curves were obtained. It was observed that the peptides were effective against both microorganisms. The effect of the peptides on growth was dose-dependent, being Osm-pepA more efficient than Osm-pepB (Fig. 3). In the case of *S. cerevisiae*, Osm-pepA presented a MIC of 40 µM, while Osm-pepB presented a MIC of 127 µM. Similar situation was observed for *P. pastoris*, although this yeast was more sensitive to Osm-pepA, as observed by the MIC value (20 µM for Osm-pepA and 127 µM for Osm-pepB). Moreover, the peptides presented a biphasic performance, promoting *S. cerevisiae* growth in low doses, 5 µM for both, and inhibiting it at doses higher than 10 µM. Analysis of the growth curve of the yeast exposed to different concentrations of peptides showed an inverted U-profile (Fig. 3A and B, inserted panels). This performance was also observed for *P. pastoris* with Osm-pepB (Fig. 3D), although it was less evident than the observed for *S. cerevisiae*.

To evaluate the effect of Osm-pepA on phytopathogenic fungi, we have tested Osm-pepA at 40 µM on spore germination of *F. solani f. sp. glycines* and *C. gossypii*. In the first case, no significant spore germination was observed in treated spores (100% inhibition), while for *C. gossypii*, some spore germination was observed, resulting in inhibition of 78% (Fig. 4).

The effect of Osm-pepA was also observed on *M. perniciosa* saprophytic hyphae. The peptide was added to PDA medium and the mycelial growth was evaluated for 13 days by accessing the mycelium diameters (Fig. 5A). It was observed that the mycelial growth rate was reduced by the presence of AMP by about 40%, considering the first 15 days (0.022 cm/day for the control and 0.013 cm/day for Osm-pepA). Besides the reduction on mycelial growth, Osm-pepA modified mycelial phenotype, causing higher hyphae density (Fig. 5B).

3.3. Tertiary structure analysis

To better understand the antimicrobial activity presented by TcOsm1 and its derived peptides, a three dimensional structural analysis was performed (Fig. 6). The TcOsm1 model presented the characteristic three-domains structure (domains I, II and III) of the antifungal PR-5. Domain I is a lectin-like β-barrel and contains 12 β-strands, domain II contains two α-helixes, and domain III presents one β-strand. Furthermore, the aminoacid residues that form the acidic cleft, and are highly conserved among the antifungal PR5

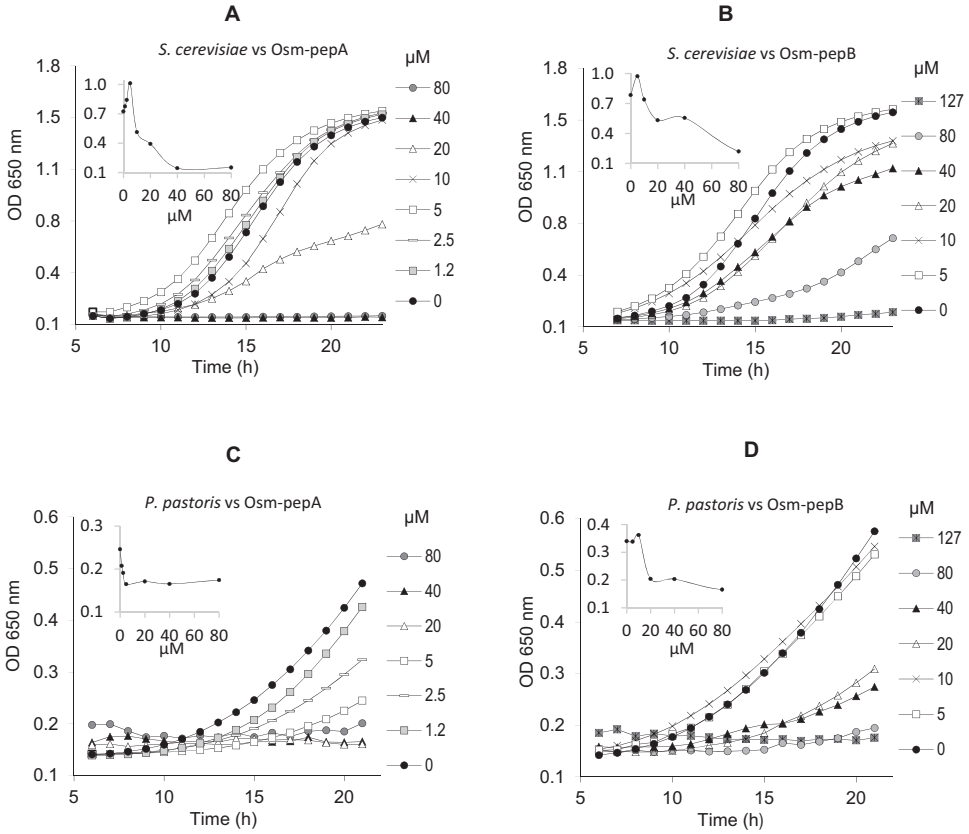

Fig. 3. Effect of TcOsm1-derived peptides, Osm-pepA and Osm-pepB, on the yeasts *Saccharomyces cerevisiae* 288c and *Pichia pastoris* X-33. Growth curves are shown between 6 and 20 h of incubation. Inserted panels: growth after 15 h of incubation with the respective peptide at different concentrations. (A) *S. cerevisiae* 288c treated with Osm-pepA. (B) *S. cerevisiae* 288c treated with Osm-pepB. (C) *P. pastoris* X-33 treated with Osm-pepA. (D) *P. pastoris* X-33 treated with Osm-pepB. The growth curves show average values from three independent experiments.

proteins (R43, E83, D96, D101, D182), were identified between domain I and II (Fig. 6A). The peptides Osm-pepA and Osm-pepB are localized in the domain I and present two β-strands (Fig. 6A). On the other hand, the molecular dynamics for the isolated peptides showed that they attain a stable conformational cluster around 6 ns (Fig. 6B), assuming a new unfolded structure, although a small segment of 3_{10}-helix can be found on Osm-pepA (Fig. 6C).

4. Discussion

Aiming to investigate the antifungal activity of cacao osmotin (TcOsm1), the mature protein was expressed in *E. coli* and the soluble fraction was used for bioassays, since this fraction usually contains the protein in the correct folding [29]. In a similar heterologous expression, a 26 kDa osmotin-like antifungal protein from *Solanum nigrum* L. was predominantly present in the soluble fraction [30]. In this work, it was initially demonstrated that TcOsm1 was present in the soluble fraction of the induced culture of pQE-osm clone, but not in the soluble fraction of the pQE-30 clone, used as a control (Fig. 1A). The osmotin-like protein was present as a fusion protein (23 kDa His-Osm fusion), and probably formed oligomers (dimers and trimers), since some higher molecular weight bands were immunologically detected in the blot. Total soluble proteins present in the supernatant of induced cultures of pQE-osm were tested against the basidiomycete *M. perniciosa,* and it was demonstrated that it caused reduction of the mycelial growth. Osmotin-like proteins from other plant species have been expressed in *E. coli* and the activity of the purified fusion proteins was evaluated. Thaumatin-like protein from *Arabidopsis* (ATLP-3) inhibited the growth of the yeast *Candida albicans* and spores germination of *Verticillium albo-atrum*, *V. dahliae*, *Fusarium*

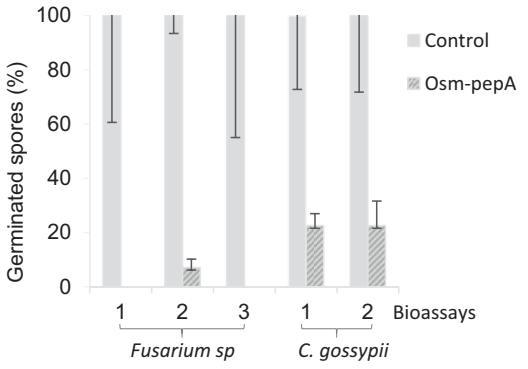

Fig. 4. Effect of Osm-pepA on the spore germination of *Fusarium solani f. sp. glycines* and *Colletotrichum gossypii*. The number of germinated spores is determined as the number of fungal colonies observed after incubation at 28 °C, for 24 h and 48 h, for *F. solani f. sp. glycines* and *C. gossypii,* respectively. Standard deviation from three replicates is indicated in each bar. The numbers 1, 2 and 3 in the x axis indicate the different bioassays for the two phytopathogens.

oxysporum, *Alternaria solani* and *Trichoderma reesei* [31]. Another example is an osmotin-like protein from *Solanum nigrum* (SnOLP) that presented antifungal activity against plant pathogenic fungi (*F. solani* f. sp. *glycines*, *Colletotrichum* spp., *Macrophomina phaseolina*) and an oomycete (*Phytophthora nicotiana var. parasitica*) under *in vitro* conditions [32]. Similarly, an osmotin isoform PcOSM2 from *Phytophthora*-resistant wild pepper (*Piper colubrinum*) presented significant inhibitory activity against *Phytophthora capsici*, which is the causal agent of the foot rot disease of black pepper, and *Fusarium oxysporum* [33].

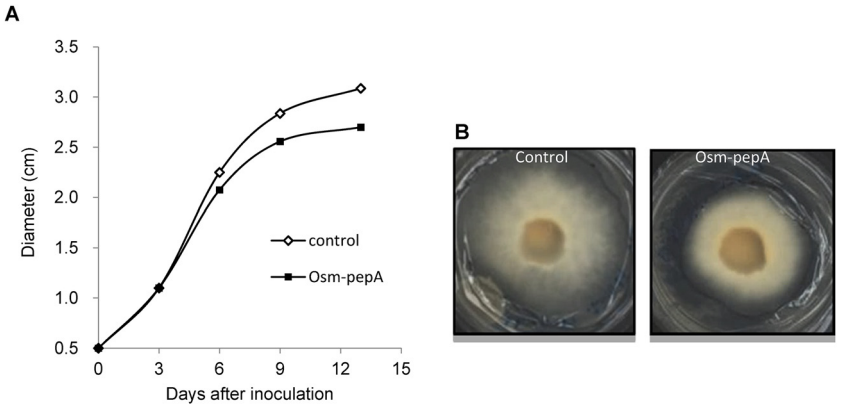

Fig. 5. Effect of Osm-pepA on *Moniliophthora perniciosa*. (A) Effect on mycelial growth. (B) Effect on mycelial phenotype after 10 days of incubation on PDA containing the 100 μM Osm-pepA. Control = Mycelium grown on PDA.

Here, we demonstrated that a soluble fraction containing a cacao osmotin (TcOsm1), expressed in *E. coli*, presented activity against the fungus *M. perniciosa*, as well as against the yeast *P. pastoris*. For more accurate analyses and comparative purposes with other reported osmotins, as well as with the derived peptides here studied, TcOsm1 must be purified and bioassayed against other phytopathogens (e.g. *F. solani f. sp. glycines* and *C. gossypii*). Furthermore, the predicted 3D structure is compatible with reported structures of other antifungal PR5 proteins, including the presence of the 5 conserved amino acid residues that form the acidic cleft, assumed to be the active site [34].

Thus, considering that cacao osmotin showed antifungal activity, we speculate whether osmotin-derived cryptic peptides with common features of AMP, such as cationic charge and a significant proportion of hydrophobic residues [11,35], could also show such activity. Two peptides were tested, Osm-pepA and Osm-pepB, and they showed antifungal activity against yeasts and filamentous fungi. They were able to inhibit the growth of both *P. pastoris* and *S. cerevisiae*, being Osm-pepA more effective than Osm-pepB. The antifungal activity of Osm-pepA, with a MIC of 20 μM for *P. pastoris* and 40 μM for *S. cerevisiae*, is comparable to that of a potent antifungal peptide, latarcin 3a, isolated from the venom of the spider *Lachesana tarabaevi*, which presented a MIC of 20 μM for both microorganisms [36]. The MIC of Osm-pepA for *S. cerevisiae* is also in the same range of the MIC of iturin (20 μM), a well-known antifungal peptide from *Bacillus subtilis* [37].

Interestingly, both peptides showed biphasic action, activating the yeast growth in lower doses and inhibiting it at higher doses.

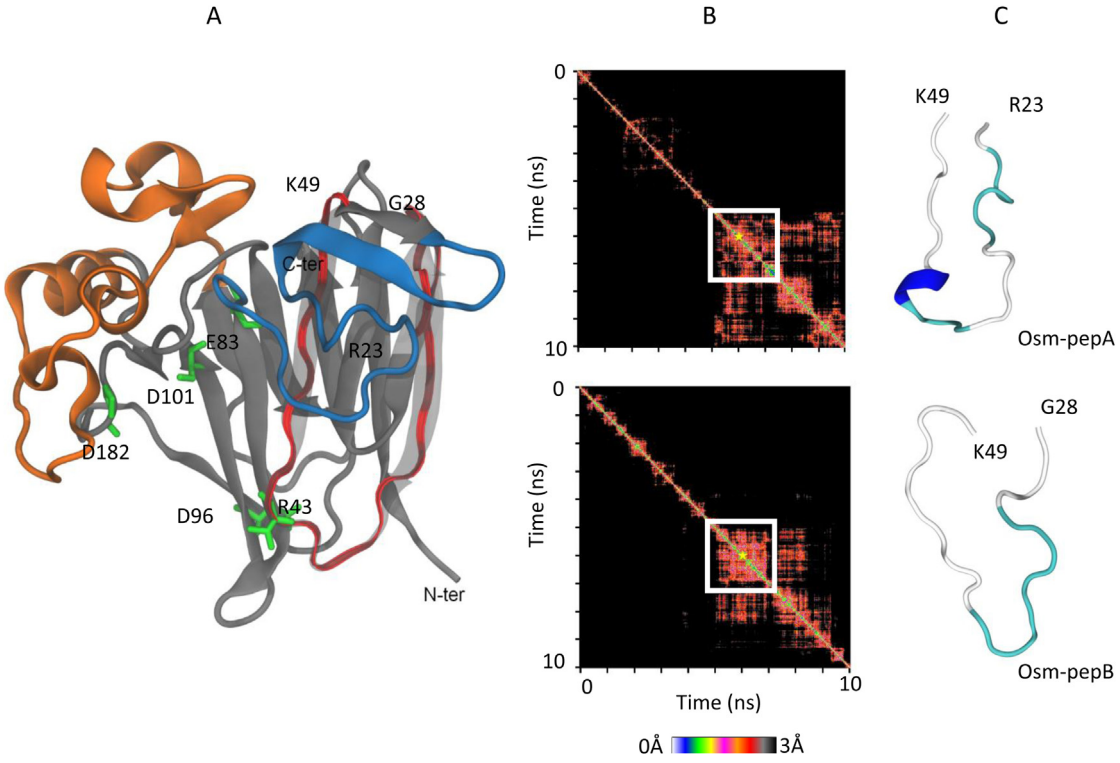

Fig. 6. Predicted 3D structure of TcOsm1 and TcOsm1-derived peptides, Osm-pepA and Osm-pepB. (A) Cartoon diagram of TcOsm1. The domains I, II and III are colored in grey, orange and blue, respectively. Conserved residues (R43, E83, D96, D101, D182) are represented in green. The region corresponding to the peptides (in red) spans from R23 to K49 (Osm-pepA) and G28 to K49 (Osm-pepB). (B) RMSD (root mean squared deviation) map showing the conformational family (white square) found during the MD simulations. (C) Representative conformation of the two peptides at 6 ns. (For interpretation of the references to colour in this figure legend, the reader is referred to the web version of this article.)

This feature is perceptible analyzing the growth curve of the yeast exposed to different concentrations of peptides, which showed an inverted U-profile (particularly, Fig. 3A and B, inserted panels). This phenomenon is called hormesis and has already been described for different compounds [38], including antimicrobial peptides [39,40].

The action of Osm-pepA was also observed in the germination of spores and hyphae growth of phytopathogenic fungi, being more effective against spores. Osm-pepA strongly inhibited the germination of spores of *F. solani f. sp. glycines* and *C. gossypii*, and mycelial growth of *M. perniciosa*. For the latter, besides the reduced radial growth, it was observed that there was a change in the mycelial phenotype that became more compact. Similar alteration in the mycelial phenotype has been described for another phytopathogenic fungus, *Magnaporthe oryzae,* the causal agent of blast disease in rice. When grown in the presence of the antifungal compound sakuranetin, a flavonoid phytoalexin, the mycelium appeared more condensed and risen on solid medium [41].

Osm-pepA and Osm-pepB differ at the N-terminus by a five amino acid residues extension, RRLDR. The structural analyses revealed that this change influenced the three dimensional peptide structure, what is probably important to its mechanism of action. In addition, it has been reported that the guanidinium group of arginine residue can interact with membrane phosphate groups by electrostatic and steric complementarity in a bidendate ligation mode, with free energies in the order of 12–15 kJ/mol, favoring peptide insertion into the hydrophobic part of the membrane [42]. Another study [43] showed that the substitution of two arginine by glycine residues and elimination of the C-terminal arginine led to the reduction of the antimicrobial activity of the peptide Protegin-1, suggesting that clusters of arginine residues may increase antimicrobial effect. The position of the arginine extension in the N-terminus of Osm-pepA is appropriate to allow its insertion in the membrane interface, giving rise to possible further investigation into this and other arginine-rich antimicrobial peptides.

The presence of these AMP encrypted in the TcOsm1 sequence raises the question of whether Osm-pepA or Osm-pepB could be released by the action of fungi or plant peptidases *in vivo*. *In silico* hydrolysis of TcOsm1 by an endopeptidase lys-C releases a large N-terminal fragment containing these peptides at its C-terminus (data not shown), but whether it occurs during plant-pathogen interaction should be investigated.

5. Conclusions

This is the first report of development of antimicrobial peptides from *T.cacao*, which were based on a pathogenesis-related (PR) protein, osmotin (TcOsm1). It was demonstrated that this protein presents antifungal activity, being effective against the yeast *P. pastoris* and one of the most important pathogens in cacao, *M. perniciosa*. The two TcOsm1-derived AMPs (Osm-pepA and Osm-pepB) were also active against yeast, a fungal model microorganism, and against the fungal phytopathogens *F. solani f. sp. glycines*, *C. gossypii* and *M. perniciosa* that are harmful to important commodities such as soybean, cotton and the cacao, respectively. These results indicate that the cacao osmotin and its derived peptides are good candidates for developing biotechnological tools aiming to control phytopathogenic fungi.

Acknowledgments

We would like to thank The National Council for Scientific and Technological Development (CNPq) and the Federal Agency for Support and Evaluation of Graduate Education (CAPES) for grants, and the Brazilian Agricultural Research Corporation (Embrapa) for financial support through project number 030864300.

References

[1] J.H. Bowers, B.A. Bailey, P.K. Hebbar, S. Sanogo, R.D. Lumsden, The impact of plant diseases on world chocolate production, Plant Health Prog. (2001), http://dx.doi.org/10.1094/PHP-2001-0709-01-RV.
[2] International Cocoa Organization, ICCO Quarterly Bulletin of Cocoa Statistics, vol. XLI, 2015.
[3] X. Argout, O. Fouet, P. Wincker, K. Gramacho, T. Legavre, X. Sabau, et al., Towards the understanding of the cocoa transcriptome: production and analysis of an exhaustive dataset of ESTs of *Theobroma cacao* L. generated from various tissues and under various conditions, BMC Genom. 9 (2008) 512, http://dx.doi.org/10.1186/1471-2164-9-512.
[4] X. Argout, J. Salse, J.-M. Aury, M.J. Guiltinan, G. Droc, J. Gouzy, et al., The genome of *Theobroma cacao*, Nat. Genet. 43 (2011) 101–108, http://dx.doi.org/10.1038/ng.736.
[5] J.M.C. Mondego, M.F. Carazzolle, G.G.L. Costa, E.F. Formighieri, L.P. Parizzi, J. Rincones, et al., A genome survey of *Moniliophthora perniciosa* gives new insights into Witches' Broom Disease of cacao, BMC Genom. 9 (2008) 548, http://dx.doi.org/10.1186/1471-2164-9-548.
[6] S. Anžlovar, M. Dermastia, The comparative analysis of osmotins and osmotin-like PR-5 proteins, Plant Biol. 5 (2003) 116–124, http://dx.doi.org/10.1055/s-2003-40723.
[7] N.K. Singh, C.A. Bracker, P.M. Hasegawa, A.K. Handa, S. Buckel, M.A. Hermodson, et al., Characterization of osmotin: a thaumatin-like protein associated with osmotic adaptation in plant cells, Plant Physiol. 85 (1987) 529–536.
[8] D. Liu, K.G. Raghothama, P.M. Hasegawa, R.A. Bressan, Osmotin overexpression in potato delays development of disease symptoms, Proc. Natl. Acad. Sci. U. S. A. 91 (1994) 1888–1892.
[9] M.L. Narasimhan, B. Damsz, M.A. Coca, J.I. Ibeas, D.J. Yun, J.M. Pardo, et al., A plant defense response effector induces microbial apoptosis, Mol. Cell 8 (2001) 921–930, S1097-2765(01)00365-3 [pii].
[10] D.J. Autelitano, A. Rajic, A.I. Smith, M.C. Berndt, L.L. Ilag, M. Vadas, The cryptome: a subset of the proteome, comprising cryptic peptides with distinct bioactivities, Drug Discov. Today 11 (2006) 306–314, http://dx.doi.org/10.1016/j.drudis.2006.02.003.
[11] N. Ueki, K. Someya, Y. Matsuo, K. Wakamatsu, H. Mukai, Cryptides: functional cryptic peptides hidden in protein structures, Biopolymers 88 (2007) 190–198, http://dx.doi.org/10.1002/Bip.20687.
[12] J. Ner, J.H. Kotlinska, J. Silberring, Crypteins—an overlooked piece of peptide systems, Curr. Protein Pept. Sci. 16 (2015) 203–218.
[13] R.E.W. Hancock, H.-G. Sahl, Antimicrobial and host-defense peptides as new anti-infective therapeutic strategies, Nat. Biotechnol. 24 (2006) 1551–1557, http://dx.doi.org/10.1038/nbt1267.
[14] C.D. Fjell, J.A. Hiss, R.E.W. Hancock, G. Schneider, Designing antimicrobial peptides: form follows function, Nat. Rev. Drug Discov. (2012), http://dx.doi.org/10.1038/nrd3653.
[15] L.T. Nguyen, E.F. Haney, H.J. Vogel, The expanding scope of antimicrobial peptide structures and their modes of action, Trends Biotechnol. 29 (2011) 464–472, http://dx.doi.org/10.1016/j.tibtech.2011.05.001.
[16] G.D. Brand, M.T.Q. Magalhaes, M.L.P. Tinoco, F.J.L. Aragao, J. Nicoli, S.M. Kelly, et al., Probing protein sequences as sources for encrypted antimicrobial peptides, PLoS One 7 (2012) e45848, http://dx.doi.org/10.1371/journal.pone.0045848.
[17] R.K. Mortimer, J.R. Johnston, Genealogy of principal strains of the yeast genetic stock center, Genetics 113 (1986) 35–43.
[18] W.C. Chan, P.D. White, Fmoc Solid Phase Peptide Synthesis: A Practical Approach, vol. 222, Oxford University Press Inc., New York, 2000.
[19] R. Subiros-Funosas, R. Prohens, R. Barbas, A. El-Faham, F. Albericio Oxyma, An efficient additive for peptide synthesis to replace the benzotriazole-based HOBt and HOAt with a lower risk of explosion, Chem. Eur. J. 15 (2009) 9394–9403, http://dx.doi.org/10.1002/chem.200900614.
[20] W.C. Chan, P.D. White, J. Beythien, R. Steinauer, Facile synthesis of protected C-terminal peptide segments by Fmoc/Bu(T) solid-phase procedures on N-Fmoc-9-Amino-Xanthen-3-Yloxymethyl polystyrene resin, J. Chem. Soc. Commun. 1995 (2016) 589–592, http://dx.doi.org/10.1039/C39950000589.
[21] M. Friedman, Applications of the ninhydrin reaction for analysis of amino acids, peptides, and proteins to agricultural and biomedical sciences, J. Agric. Food Chem. 52 (2004) 385–406, http://dx.doi.org/10.1021/Jf030490p.
[22] D. Suckau, A. Resemann, M. Schuerenberg, P. Hufnagel, J. Franzen, A. Holle, A novel MALDI LIFT-TOF/TOF mass spectrometer for proteomics, Anal. Bioanal. Chem. 376 (2003) 952–965, http://dx.doi.org/10.1007/s00216-003-2057-0.
[23] J.B. Murphy, M.W. Kies, Note on spectrophotometric determination of proteins in dilute solutions, Biochim. Biophys. Acta 45 (1960) 382–384, http://dx.doi.org/10.1016/0006-3002(60)91464-5.
[24] M.M. Bradford, A rapid and sensitive method for the quantitation of microgram quantities of protein utilizing the principle of protein-dye binding, Anal. Biochem. 72 (1976) 248–254.
[25] U.K. Laemmli, Cleavage of structural proteins during the assembly of the head of bacteriophage T4, Nature 227 (1970) 680–685.

[26] J. Sambrook, E.F. Fritsch, T. Maniatis, Molecular Cloning: A Laboratory Manual, Cold Spring Harbor Laboratory Press, 1989.
[27] C.-C. Chen, J.-K. Hwang, J.-M. Yang, (PS) 2: protein structure prediction server, Nucleic Acids Res. 34 (2006) W152–W157, http://dx.doi.org/10.1093/nar/gkl187.
[28] J.C. Phillips, R. Braun, W. Wang, J. Gumbart, E. Tajkhorshid, E. Villa, et al., Scalable molecular dynamics with NAMD, J. Comput. Chem. 26 (2005) 1781–1802, http://dx.doi.org/10.1002/jcc.20289.
[29] S. Ventura, A. Villaverde, Protein quality in bacterial inclusion bodies, Trends Biotechnol. 24 (2006) 179–185, http://dx.doi.org/10.1016/j.tibtech.2006.02.007.
[30] S. Chowdhury, A. Basu, S. Kundu, Cloning, characterization, and bacterial over-expression of an osmotin-like protein gene from *Solanum nigrum* L. with antifungal activity against three necrotrophic fungi, Mol. Biotechnol. 57 (2015) 371–381, http://dx.doi.org/10.1007/s12033-014-9831-4.
[31] X. Hu, A.S. Reddy, Cloning and expression of a PR5-like protein from *Arabidopsis*: inhibition of fungal growth by bacterially expressed protein, Plant Mol. Biol. 34 (1997) 949–959.
[32] M.A. Campos, M.S. Silva, C.P. Magalhaes, S.G. Ribeiro, R.P. Sarto, E.A. Vieira, et al., Expression in *Escherichia coli*, purification, refolding and antifungal activity of an osmotin from *Solanum nigrum*, Microb. Cell Fact. 7 (2008) 7, http://dx.doi.org/10.1186/1475-2859-7-7, 1475-2859-7-7 [pii].
[33] T. Mani, K.C. Sivakumar, S. Manjula, Expression and functional analysis of two osmotin (PR5) isoforms with differential antifungal activity from piper colubrinum: prediction of structure–function relationship by bioinformatics approach, Mol. Biotechnol. 52 (2011) 251–261, http://dx.doi.org/10.1007/s12033-011-9489-0.
[34] J.J. Liu, R. Sturrock, A.K. Ekramoddoullah, The superfamily of thaumatin-like proteins: its origin, evolution, and expression towards biological function, Plant Cell Rep. 29 (2010) 419–436, http://dx.doi.org/10.1007/s00299-010-0826-8.
[35] M. Torrent, M.V. Nogues, E. Boix, Discovering new In silico tools for antimicrobial peptide prediction, Curr. Drug Targets 13 (2012) 1148–1157.
[36] S.A. Kozlov, A.A. Vassilevski, A.V. Feofanov, A.Y. Surovoy, D.V. Karpunin, E.V. Grishin, Latarcins, antimicrobial and cytolytic peptides from the venom of the spider *Lachesana tarabaevi* (Zodariidae) that exemplify biomolecular diversity, J. Biol. Chem. 281 (2006) 20983–20992, http://dx.doi.org/10.1074/jbc.M602168200.
[37] L. Thimon, F. Peypoux, J. Wallach, G. Michel, Effect of the lipopeptide antibiotic, iturin A, on morphology and membrane ultrastructure of yeast cells, FEMS Microbiol. Lett. 128 (1995) 101–106, http://dx.doi.org/10.1111/j.1574-6968.1995.tb07507.x.
[38] E.J. Calabrese, R.B. Blain, The hormesis database: the occurrence of hormetic dose responses in the toxicological literature, Regul. Toxicol. Pharmacol. 61 (2011) 73–81, http://dx.doi.org/10.1016/j.yrtph.2011.06.003.
[39] W.A. Reed, K.L. White, F.M. Enright, J. Holck, J.M. Jaynes, G.W. Jeffers, Enhanced in vitro growth of murine fibroblast cells and preimplantation embryos cultured in medium supplemented with an amphipathic peptide, Mol. Reprod. Dev. 31 (1992) 106–113, http://dx.doi.org/10.1002/mrd.1080310204.
[40] S.A. Kuckelhaus, J.R. Leite, M.I. Muniz-Junqueira, R.N. Sampaio, C. Bloch Jr., C.E. Tosta, Antiplasmodial and antileishmanial activities of phylloseptin-1, an antimicrobial peptide from the skin secretion of *Phyllomedusa azurea* (Amphibia), Exp. Parasitol. 123 (2009) 11–16, http://dx.doi.org/10.1016/j.exppara.2009.05.002.
[41] M. Hasegawa, I. Mitsuhara, S. Seo, K. Okada, H. Yamane, T. Iwai, et al., Analysis on blast fungus-responsive characters of a flavonoid phytoalexin sakuranetin; accumulation in infected rice leaves, antifungal activity and detoxification by fungus, Molecules 19 (2014) 11404–11418, http://dx.doi.org/10.3390/molecules190811404.
[42] K.A. Schug, W. Lindner, Noncovalent binding between guanidinium and anionic groups: focus on biological- and synthetic-based arginine/guanidinium interactions with phosph[on]ate and sulf[on]ate residues, Chem. Rev. 105 (2005) 67–113, http://dx.doi.org/10.1021/Cr040603j.
[43] M. Tang, A.J. Waring, M. Hong, Effects of arginine density on the membrane-bound structure of a cationic antimicrobial peptide from solid-state NMR, Biochim. Biophys. Acta Biomembr. 1788 (2009) 514–521, http://dx.doi.org/10.1016/j.bbamem.2008.10.027.